

Laser Welding and Heat Treatment of Steel 0H15N7M2J

Abstract: The article presents the results of tests concerning the mechanical and structural properties of single-spot and twin-spot laser beam welded joints made of a steel strip, the chemical composition of which corresponds to that of steel 0H15N7M2J. In addition, the article presents the comparison concerning the geometry of joints made using the single and twin-spot laser beam. The test joints were subjected to heat treatment involving austenitisation, cold treatment and ageing. The study also involved the comparison of the mechanical and structural properties of the joints subjected and those not subjected to the above named heat treatment.

Keywords: laser welding, steel 0H15N7M2J, welding tests, joint properties

DOI: [10.17729/ebis.2016.4/5](https://doi.org/10.17729/ebis.2016.4/5)

Introduction

Precipitation hardened corrosion resistant martensitic steels, often referred to in scientific publications as controlled transformation steels, combine good strength characteristic of martensitic structures with good ductility, usually characteristic of austenitic steels. One of such steels is steel 0H15N7M2J according to PN-EN 10088-2:2005, characterised by high fatigue strength, excellent corrosion resistance, plastic workability and small strains accompanying heat treatment. In the supersaturated state, the steel structure is austenitic. Only after long cold treatment at a temperature below 78°C is it possible to obtain a martensitic-austenitic structure. Further hardening of the steel is obtained through ageing at a temperature ensuring the dispersive precipitation of intermetallic phases in the matrix, leading to the significant increase in mechanical properties.

The above-presented steel is used when making sheets/plates, rods and wires, out of which high strength corrosion resistant elements are manufactured [1-4].

Laser welding is the process of joining metals, during which heat necessary for melting a given material is obtained by absorbing the monochromatic electromagnetic wave. The possibility of obtaining considerable power density at an area where a laser beam is focused (high laser beam power over a very small area) is responsible for the fact that welds obtained through keyhole welding are relatively narrow and deep, whereas the area of the heat affected zone (HAZ) is very limited. Very high metal heating and melting rates as well as equally fast cooling are responsible for the fact that both the weld and the HAZ do not reveal any significant grain growth and structural changes may significantly differ from those occurring during

dr inż. Maciej Róžański (PhD (DSc) Eng.); dr inż. Sebastian Stano (PhD (DSc) Eng.) – Instytut Spawalnictwa, Welding Technologies Department; dr hab. inż. Adam Grajcar (PhD (DSc) Hab. Eng.) – Silesian University of Technology; Division of Constructional and Special Materials

arc welding processes. In some cases, it is convenient to split the laser beam into two component beams focused at two different points (bifocal welding). Depending on the distance between each other, the beams can form a common wider gasodynamic channel or two separate channels, thus affecting the solidification of metal and structural changes, if any. The focusing of the beam at two points in the tandem system reduces the cooling rate of elements during welding, may reduce welding stresses, and, in cases of materials susceptible to hardening, could temper the martensitic structure or prevent entire hardening [5-7].

The work involved tests concerning the effect of single-spot and twin-spot laser beam welding on the structure and mechanical properties obtained directly after welding and after treatment involving hardening, cold treatment and ageing.

Test Materials

The tests concerned the effect of laser welding parameters on the properties of joints made of precipitation hardened martensitic-austenitic steel 0H15N7M2J. The test joints were made using 0.8 mm thick, 65 mm wide and 100 mm long strips of the steel in the supersaturated state.

The tests also involved the verification of chemical composition using spark source optical emission spectrometry and a Q4 TASMAN spectrometer manufactured by Bruker. The chemical composition test results are presented

in Table 1. In addition, the tests concerned the mechanical properties of the strip used. The results of the above named tests are presented in Table 2.

Test Joints

The welding tests involving the above named steel were performed using the keyhole welding technique, a solid state laser, integrated with a robotic system for laser processing, installed at Instytut Spawalnictwa in Gliwice (Fig. 1). The welding station was equipped as follows:

- Laser TruDisk 12002 – a Yb:YAG solid-state laser (Trumpf) having a maximum power of 12 kW and laser beam quality designated by the parameter of $BPP \leq 8 \text{ mm}\cdot\text{mrad}$ (Fig. 1a)
- CFO head (Trumpf) used for single-spot laser welding (Fig. 1b). The head was connected to the laser source using an optical fibre having a diameter of 200 μm and a focusing lens having a focal length of $f_{\text{og}} = 300 \text{ mm}$. The diameter of the laser beam focus amounted to 300 μm .
- D70 head (Trumpf) provided with a system enabling the twin-spot focusing of a laser beam (Fig. 1c); the head was connected to the laser source using an optical fibre having a diameter of 600 μm and a focusing lens having a focal length of $f_{\text{og}} = 200 \text{ mm}$; the diameter of a single laser beam focus amounted to 600 μm .

The distribution of power density (laser beam power distribution) between two focuses was

Table 1. Chemical composition of the steel used in the tests – chemical analysis result

Steel designation	Chemical composition, % by weight								
	C	Si	Mn	Cr	Mo	Ni	Cu	Co	Al
0H15N7M2J	0.024	0.16	1.41	17.14	2.14	9.1	0.22	0.084	0.89

Table 2. Mechanical properties of the strip in the supersaturated state corresponding in terms of chemical composition to steel 0H15N7M2J

Designation of tested steel equivalent	Tensile strength R_m , MPa	Yield point R_e , MPa	Elongation A_5 , %
0H15N7M2J	1030	804	23,9

Note: values averaged from three measurements

monitored using a UFF100 laser beam analyser manufactured by Prometec (Fig. 1c). The shielding gas (Ar) was blown via a side nozzle at a flow rate of 12 l/min.

As regards the D70 head, the twin-spot laser beam is obtained by placing a special optical module across the laser beam, thus splitting the beam and changing its trajectory. Afterwards, the beam is focused on two spots by standard focusing lenses, as in classical laser welding. The distance between the focuses of the laser beam is affected by the inclination of the optical module plane. The laser beam power distribution is influenced by the position of the optical module in relation to the laser beam. The maximum distance between the beam focuses adopted when making the test joints amounted to 4 mm, i.e. the maximum distance available for the head used in the tests (D70). It was assumed that the tests would be performed with a beam power distribution of 50:50 and 60:40 (the first value defines the percentage fraction of beam power in the pilot focusing point of the tandem system). The change in power density distribution consisted in the manual change in the position of the optical module in relation to the laser beam. Each change in the above named position entailed a change in power distribution between individual focuses and in each case was verified by measuring density distribution between the two focuses. In the tests, the verification of the actual power density distribution was performed using the UFF100 laser beam analyser manufactured by Prometec. The graphic representation concerning the results of the measurement related to the power distribution of the twin-spot laser beam is shown in Figure 2.

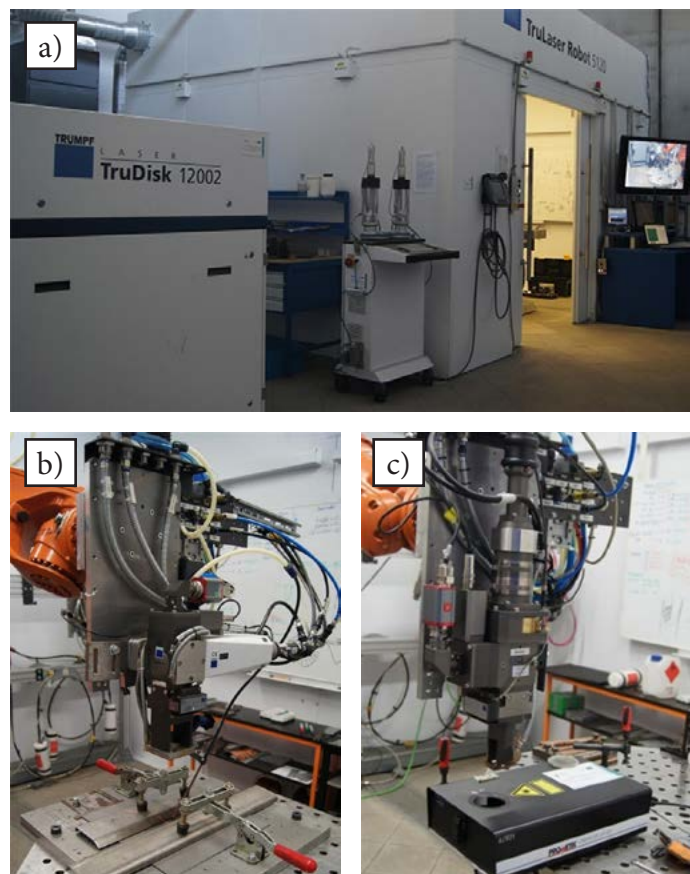


Fig. 1. TruDisk 12002 disc laser integrated with the robotic station. Main view (a), CFO head for keyhole welding (b), D70 head with the bifocal system fixed to the wrist of the industrial robot and the UFF100 laser beam analyser (c)

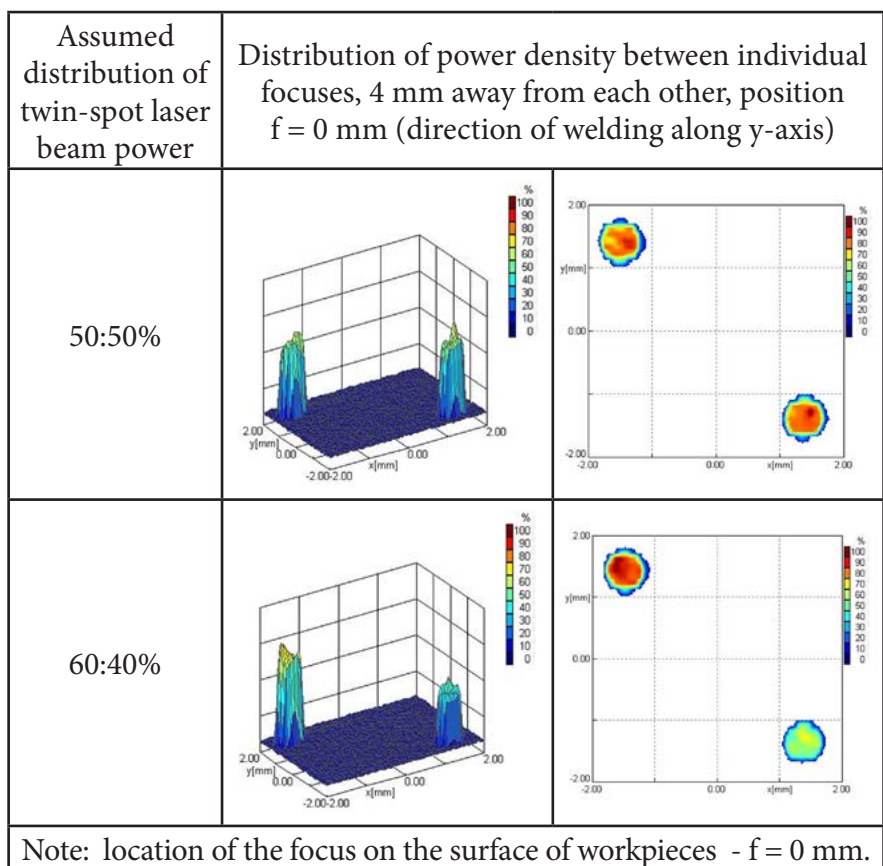


Fig. 2. Graphic presentation of twin-spot laser beam power distribution, performed using a UFF100 device manufactured by Prometec

In order to determine the effect of single and twin-spot laser welding parameters on the mechanical properties and the structure of 0.8 mm thick butt joints made of steel 0H15N7M2J, it was necessary to make test joints using various sets of process parameters. The initial tests enabled the selection of 3 sets of single-spot laser welding parameters (Table 3) and 4 sets of twin-spot laser welding parameters (Table 4). Parameters were selected in a manner ensuring the obtainment of the proper quality of joints (according to adopted parameters), i.e. with the penetration across the entire thickness of the base material and without spatters, burn-throughs, undercuts etc.

Visual Tests

The making of the test joints was followed by their visual inspection performed in accordance with standard PN-EN ISO 17637:2011E *Non-destructive tests of welds. Visual testing of fusion-welded joints*. The tests aimed to determine the correctness of weld geometry and to enable the selection of joints for further tests by eliminating those failing to meet the requirements of quality level B according to PN-EN ISO 13919-1 *Welding. Electron and laser beam welded joints. Guidance on quality levels for imperfections. Steel*.

Table 3. Parameters of the single-spot laser beam welding of 0.8 mm thick sheets made of steel 0H15N7M2J

Specimen no.	11	12	13
Beam power, kW	1.5	2.5	4.5
Welding rate, cm/min	350	780	1500
Linear energy, kJ/mm	0.0257	0.0187	0.0180

Table 4. Parameters of the twin-spot laser beam welding of 0.8 mm thick sheets made of steel 0H15N7M2J

Specimen no.	21	22	23	24
Beam power, kW	4	4	3	3
Welding rate, cm/min	1080	1080	840	840
Beam power distribution, %	50:50	60:40	50:50	60:40
Linear energy, kJ/mm	0.039	0.039	0.035	0.035

Joints nos. 11 and 12 (welding parameters - Table 3) revealed the entire penetration across the thickness of the base material; the geometry of the weld face and of the weld root was unchanged along the entire length. Joint no. 13 revealed local burn-throughs and spatters in the welded joint area. Despite the foregoing, the latter joint was also selected for macro and microscopic metallographic tests as well as for cross-sectional hardness measurements. All of the twin-spot laser beam welded joints (Table 4) revealed the entire penetration of the base material and the unchanged and proper geometry of the weld face and weld root along the entire length of the joint. All of the joints revealed the depletion of weld metal, which was probably caused by the evaporation of steel components characterised by high vapour pressure at welding temperature. Because of the thickness of the sheets being welded (0.8 mm), the visual inspection concerning the depletion of weld metal and the measurement of possible dimensions of characteristic welding imperfections, such as undercuts or the incomplete filling of the weld groove and qualifying such observed imperfections as representing a given quality level according to standard PN-EN ISO 13919-1 was very difficult. The assessment of the quality of the joints was possible only after performing macroscopic metallographic tests.

Heat Treatment of Laser Welded Joints Made of Steel 0H15N7M2J

The obtainment of appropriately high mechanical properties of precipitation hardened high-alloy austenitic steels is ensured by properly performed heat treatments. As regards the tested high-alloy steel corresponding, in terms of the chemical composition, to steel 0H15N7M2J, in accordance with the steel data sheet, the process of heat treatment consisted in 1-hour long austenitisation at a temperature 950°C, cooling in oil, 1-hour long cold treatment at a temperature of -80°C and 3-hour long

ageing at a temperature of 510°C. As regards the single-spot laser beam welded joints, the heat treatment involved joints nos. 11, 12 and 13 (welding parameters – Table 3). In terms of the twin-spot laser beam welded joints, the heat treatment involved all of the welded joints (welding parameters – Table 4).

The process of heat treatment was performed in the laboratory of Testing of Materials Weldability and Welded Constructions Department at Instytut Spawalnictwa. The heat treatment process is presented in Figure 3.

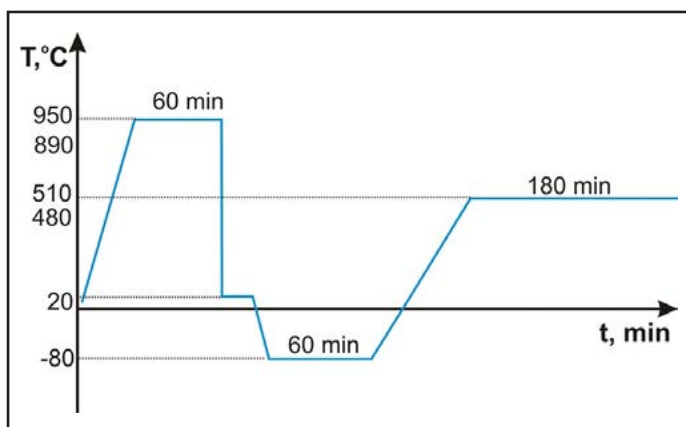


Fig. 3. Scheme of the temperature-time parameters used during the heat treatment of steel 0H15N7M2J

Metallographic Tests

Macroscopic Metallographic Tests

The structure of the welded joints made of steel 0H15N2M2J was revealed by electrolytic etching. The macroscopic metallographic tests were performed using a Nikon Eclipse MA200 light microscope. The macroscopic metallographic tests were performed using all of the selected sets of parameters. The macrostructures of the single-spot laser beam welded joint made of steel 0H15N7M2J are presented in Figure 4, whereas those of the twin-spot laser beam welded joint are presented in Figure 5.

As regards the single-spot laser beam welded joints, the decrease in welding linear energy from 0.0257 kJ/cm to approximately 0.0180 kJ/cm only slightly affected the width of the weld. In turn, the geometry of the welded joints was

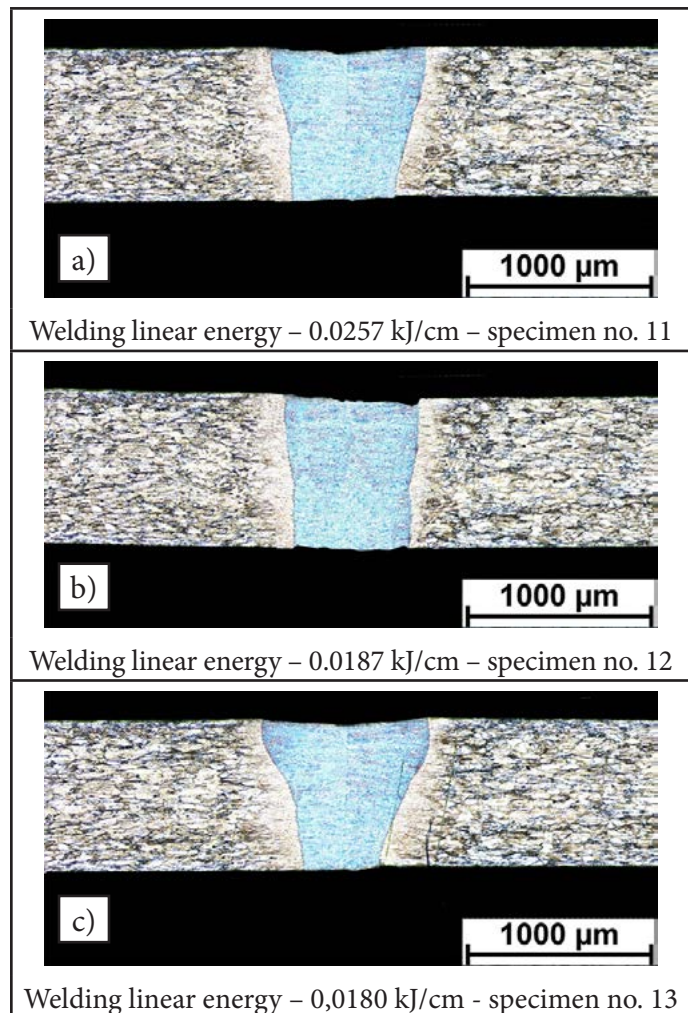


Fig. 4. Macrostructure of the single-spot laser beam welded joints made of steel 0H15N7M2J using a linear energy of 0.0257 kJ/cm – specimen no. 11 (a), 0.0187 kJ/cm – specimen no. 12 (b) and 0.0180 kJ/cm – specimen no. 13 (c)

significantly influenced by the welding rate. In the case of the welded joint made using a welding rate of 350 cm/min (Fig. 4a) and 780 cm/min (Fig. 4b), the welds revealed almost parallel fusion lines, which reduced stresses in the weld and minimised the angular strain of the joint. After increasing a welding rate to 1500 cm/min (Fig. 4c), the weld geometry changed significantly; the volume of the crystallising metal of the weld above its neutral axis was significantly greater than the volume of the weld metal below the axis. The areas of the single-spot laser beam welded joints subjected to the macrostructural tests did not reveal welding imperfections disqualifying the joints as made improperly.

The twin-spot laser beam welded joints made of steel 0H15N7M2J did not reveal the significant

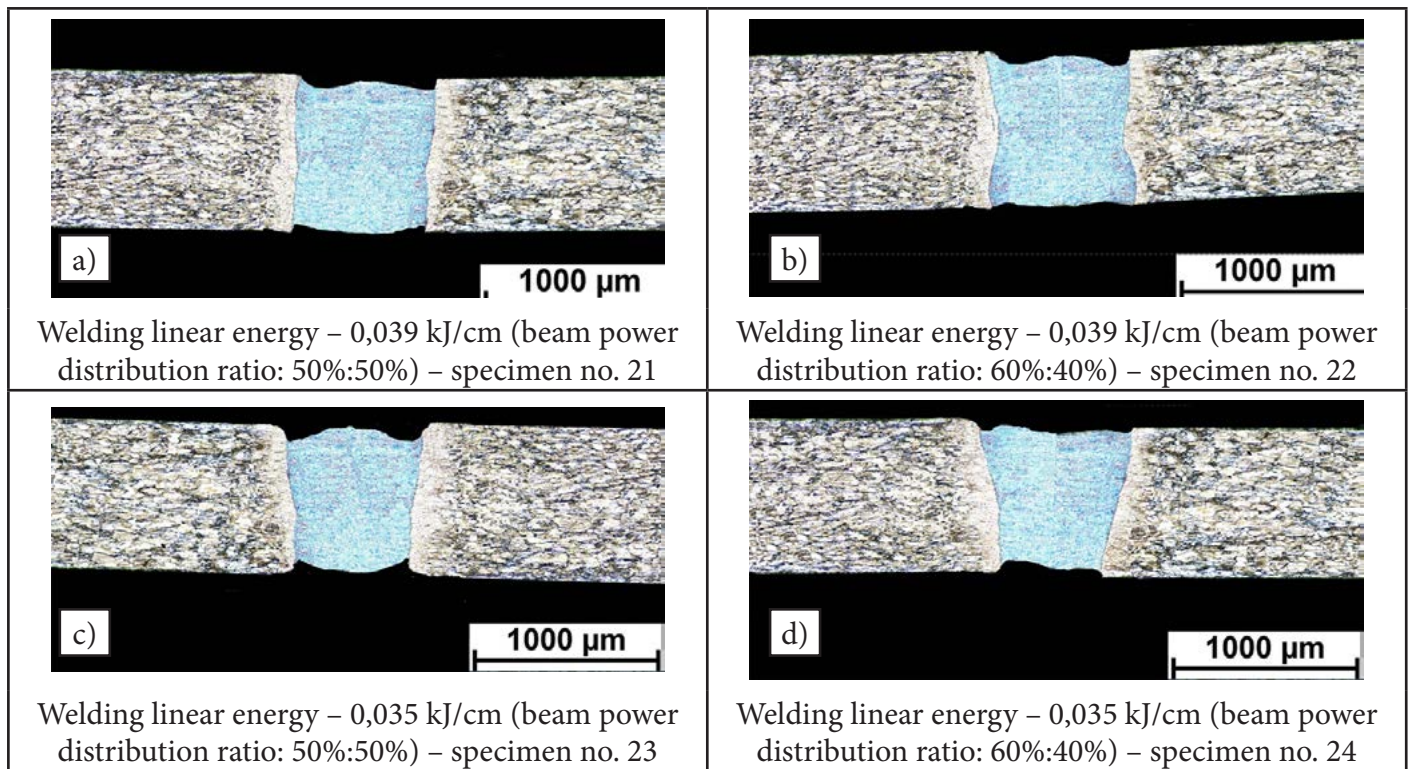


Fig. 5. Macrostructure of the twin-spot laser beam welded joints made of steel 0H15N7M2J using a linear energy of 0.039 kJ/cm with the beam power distribution ratio of 50%:50% - specimen no. 21 (a), using a linear energy of 0.039 kJ/cm with the beam power distribution ratio of 60%:40% - specimen no. 22 (b), using a linear energy of 0.035 kJ/cm with the beam power distribution ratio of 50%:50% - specimen no. 23 (c) and using a linear energy of 0.035 kJ/cm with the beam power distribution ratio of 60%:40% - specimen no. 24 (d)

effect of the laser beam power distribution (between the focuses) on the joint geometry. However, in each case (Fig. 5a-d), numerous welding imperfections (undercuts) were observed; the imperfections were restricted within quality level B according to standard PN-EN ISO 13919-1. In addition, the twin-spot laser beam welded joints revealed a decrease in the active cross-section of the joint caused by the depletion of the weld metal. It should be emphasized that the significant depletion of the weld metal, decreasing the active cross-section of the joint, undoubtedly reduced its strength.

Microscopic Metallographic Tests

Similar to the macroscopic tests, the microscopic metallographic tests of the welded joints were performed using a Nikon Eclipse MA200 metallographic light microscope. The microstructural observations involved the base material and the welded joint, i.e. the weld and the heat affected zone. The tests were performed on the joints made using the single-spot laser

beam having a linear energy of 0.018 kJ/cm in the state before and after the heat treatment. The test results are presented in Figure 6 and 7.

As regards the welded joint made of steel 0H15N7M2J in the pre-heat-treatment state, the weld material was the dendritic mixture of austenite with ferrite delta (Fig. 6c). In turn, the base material structure contained strain-induced austenite with numerous slide lines, strain bands and some amounts of martensite (Fig. 6b). The strain effects were not visible or only slightly visible in the heat affected zone; the content of martensite was close to 0, the slide lines and bands were hardly visible (Fig. 6d). The structure of the base material contained few coagulated precipitates (Fig. 6d), affecting the steel hardening to a very little degree.

The heat treatment of the welded joint significantly changed the microstructure of the joints and of the base material. The base material microstructure was almost entirely composed of austenite; the chemical composition might also include some amount of ferrite delta) (Fig.

7b). The base material contained numerous dispersive precipitates. Taking into consideration the chemical composition of the steel and the effect of the heat treatment, it could be supposed that precipitated particles were $M_{23}C_6$ carbides and intermetallic phases such as Ni_3Mo , Fe_2Mo , $(Fe,Ni)_2Mo$, Ni_3Al and $NiAl$. The supposition needs to be fully confirmed using more detailed X-ray tests as well as the accurate analysis of the chemical composition of precipitates using energy dispersive spectrometry (EDS). The structure of the weld subjected to the heat treatment was the mixture of martensite (formed after cold treatment) as well as ferrite delta and other precipitates. The detailed analysis of the above named precipitates will be the subject of further studies (Fig. 7c). In addition, the fusion line (Fig. 7d) contained chain-like precipitates of hardening phases. Such an arrangement of hard phases can significantly reduce joint plasticity and even lead to joint brittleness.

Tensile Tests

The tensile tests involved the single-spot laser beam welded joint made using the set of parameters no. 12 in Table 3 and the twin-spot laser beam welded joint made using the set of parameters no. 22 in Table 4. The tensile tests involved both the specimens directly after welding (not subjected to the heat treatment) and those subjected to the heat treatment. The tensile tests were performed using a testing machine (model 4210) manufactured by Instron.

Specimens for the tensile tests were prepared in accordance with the requirements specified in standard PN-EN ISO 4163:2013. Each of the joints was subjected to 3 tensile tests. The tensile test results are presented in Table 5 and Figure 8.

The tensile test results revealed that both as regards the single and twin-spot laser beam

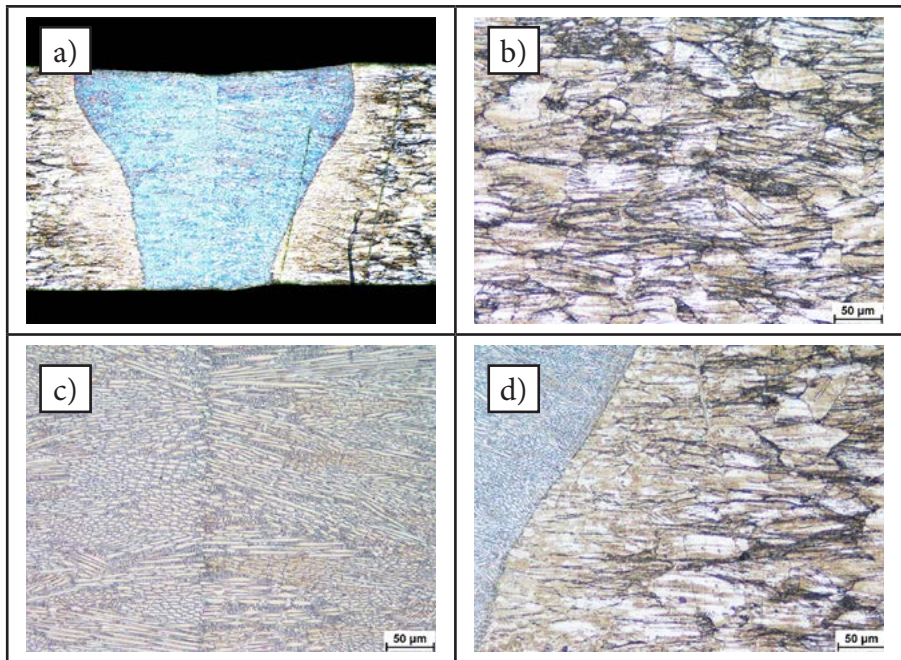


Fig. 6. Macro and microstructure of the joint made of steel 0H15N7M2J using a linear energy of 0.0180 kJ/cm in the state before and after the heat treatment: joint macrostructure (a), base material microstructure (b), weld (c) fusion line and HAZ (d)

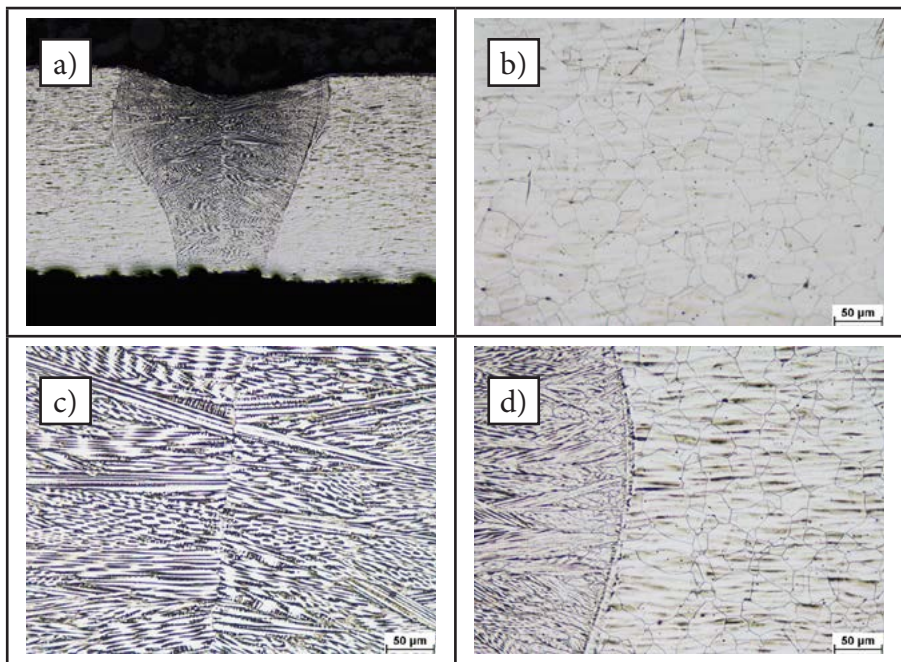


Fig. 7. Macro and microstructure of the single-spot laser beam welded joint made of steel 0H15N7M2J using a linear energy of 0.0180 kJ/cm in the state after the heat treatment: joint macrostructure (a), base material microstructure (b), weld (c) fusion line and HAZ (d)

Table 5. Tensile test results related to the joints made of steel 0H15N7M2J, laser welded using the single-spot (no. 12) and twin-spot beam (no. 22)

Specimen (Table 3 and 4)	Heat Treatment	Tensile strength, R_m MPa			Average, R_m MPa	Standard deviation MPa
		1	2	3		
12	No	610	562	584	585	24.1
12	Yes	984	1027	999	1003	21.8
22	No	541	572	529	547	22.2
22	Yes	978	953	942	958	18.4

Note: In each case, the specimen ruptured in the weld

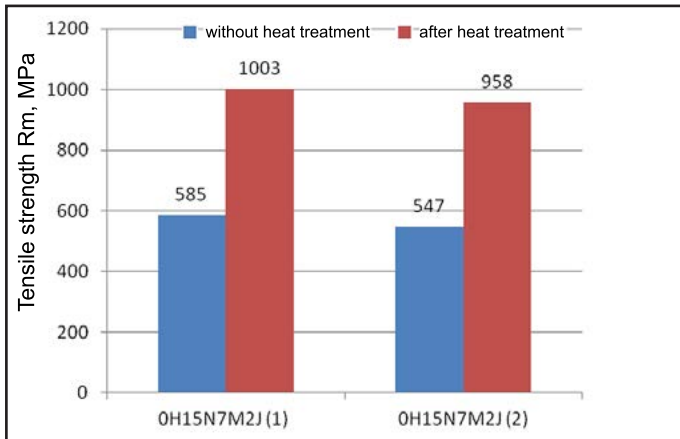


Fig. 8. Tensile strength of the single-spot (1) and twin-spot (2) laser beam welded joints made of steel 0H15N7M2J not subjected and subjected to the heat treatment



Fig. 9. Photographs of the exemplary laser-beam welded specimen after the tensile strength test – rupture in the weld

welded joints, the test specimens ruptured in the weld (Fig. 9), which means that in each case the strength of the welded joint was lower than that of the base material, both as regards the joints subjected to the heat treatment and those which remained in the state directly following the welding process. The tensile strength of the single-spot laser beam welded joints directly after welding amounted to 585 MPa, constituting approximately 56% of the base material hardness (Table 2, Table 5). The tensile strength of

the same joints subjected to the heat treatment amounted to 1003 MPa, constituting approximately 97% of the base material hardness. In turn, the tensile strength of the twin-spot laser beam welded joint not subjected to additional heat treatment amounted to 547 MPa, constituting approximately 53% of the base material hardness, whereas the tensile strength of the twin-spot laser beam welded joint subjected to the heat treatment amounted to 958 MPa, constituting approximately 93% of the base material hardness. Therefore, it can be assumed that it is possible to make a weld characterised by tensile strength similar to that of the base material. It should be noted that the weld geometry always constitutes a geometrical notch (depletion of metal on the weld face side) leading to the accumulation of stressed in the transition area between the weld face and the base material.

Cross-Sectional Hardness Measurements of Welded Joints

Cross-sectional hardness measurements of the welded joints were performed by means of a KB50BVZ-FA testing machine manufactured by KB Prüftechnik, using an indenter load of 9.81 N (HV1). Hardness was measured in both directions from the weld axis. The distance between measurement points amounted to 0.2 mm and the measurement line was located in the middle of the weld thickness. Hardness tests only involved the single-spot laser beam welded joints in relation to each set of welding parameters used. Hardness tests involved both the joints subjected and not subjected to the

heat treatment. The primary objective concerning cross-sectional hardness measurements of the welded joints was to determine the effect of the welding process on changes in the hardness of the welded joints as well as to identify the effect of the heat treatment and precipitation processes on the hardness increase in the individual areas of the welded joints. Cross-sectional hardness measurements involving the twin-spot laser beam welded joints were omitted as changes in the width of the weld and that of the heat affected zone do not affect hardness. The results of the hardness tests involving the single-spot laser beam welded joints are presented in Figure 10.

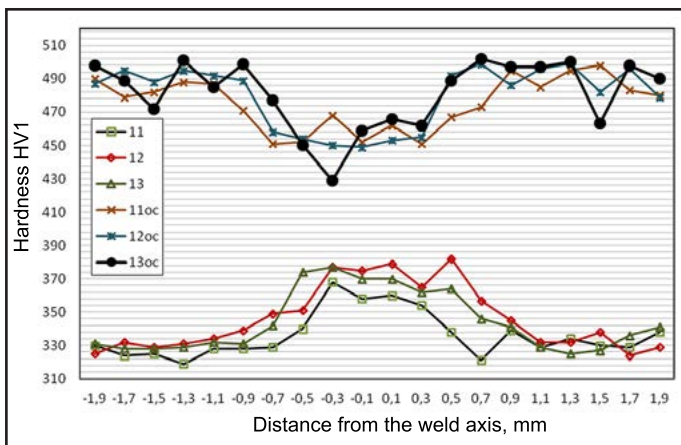


Fig. 10. Results of the cross-sectional hardness measurements of the single-spot laser beam welded joints made of steel 0H15N7M2J before (11-13) and after the heat treatment (11oc-13oc)

The cross-sectional hardness measurement of the single-spot laser beam welded joints made of steel 0H15N7M2J revealed that the process of welding increased the hardness of the weld metal if compared with that of the base material. The hardness of the base material amounted to 315-343 HV1 and increased in the weld metal to approximately 360-375 HV1, where the direct effect of welding linear energy on the increase in the weld metal hardness was not observed. The significant increase in the hardness of both the base material and the weld was caused by the heat treatment. After the heat treatment, the hardness of the base

material increased to 470-505 HV1, i.e. by more than 150 HV1. This could be attributed to the precipitation process taking place during ageing and the precipitation of numerous hardening phases, the identification of which will be possible after the use of X-ray and microscopic techniques of greater resolution. The hardness of the weld increased to a lesser degree, i.e. to 430-470 HV1, by approximately 100 HV1 in relation to the hardness of the welded joint preceding the heat treatment.

Conclusions

1. Single and twin-spot laser beam welding enables the obtainment of high-quality joints of thin-walled elements made of steel 0H15N7M2J.
2. The heat treatment of laser welded joints made of steel 0H15N7M2J leads to the precipitation of dispersive phases in the austenitic matrix.
3. The tensile strength of the single and twin-spot laser beam welded joints not subjected to further heat treatment amounts to 585 MPa and 547 MPa respectively, i.e. 53% and 56% of the base material in the as-delivered state. The heat treatment of the joints increases the tensile strength to a tensile strength value close to that of the base material, i.e. to 1003 MPa and 958 MPa respectively, constituting 97% and 93% of the base material tensile strength. Such significant hardening is caused by the occurrence of precipitation phenomena.
4. The heat treatment of laser welded joints made of steel 0H15N7M2J increases the hardness of the base material from approximately 300 HV1 to approximately 500 HV1 and that of the weld from approximately 370 HV1 to approximately 450 HV1, which can be attributed to the effect of precipitation hardening.
5. Single-spot laser beam welding causes the less intense evaporation of the weld metal than that accompanying twin-spot laser beam welding.

References

- [1] Blicharski M.: *Inżynieria materiałowa. Stal*. WNT, Warszawa, 2004.
- [2] Pawlak S.J.: *Austenite stability in the high strength metastable stainless steel*. Journal of Achievements in Materials and Manufacturing Engineering, 2007, vol. 22, issue 2.
- [3] *Charakterystyki stali seria E*, vol. II. Instytut Metalurgii Żelaza im. S. Staszica w Gliwicach
- [4] Ozgowicz W., Kurc-Lisiecka A., Grajcar A.: *Corrosion behaviour of cold-deformed austenitic alloys*. [in]: Valdez Salas B., Schorr M. (eds.): *Environmental and industrial corrosion – practical and theoretical aspects* InTech, Rijeka, 2012, chapter 4, pp. 79-107
- [5] Banasik M., Stano S., Polak J.: *Possibility of using Nd:YAG laser for precise joining of thin-walled elements of structures on the example of the flow sensor pitot probe*. Welding International, 2013, vol. 27, issue 6. <http://dx.doi.org/10.1080/09507116.2011.606139>
- [6] Pilarczyk J., Stano S., Banasik M., Dworak J.: *Wykorzystanie technik laserowych do spawania elementów o małych wymiarach w Centrum Laserowym Instytutu Spawalnictwa. Problemy Eksploatacji. Zeszyty Naukowe Instytutu Technologii Eksploatacji – PIB*, 2011, no. 4.
- [7] Różański M., Grajcar A., Stano S.: *Wpływ energii liniowej spawania wiązką laserową na mikrostrukturę i wybrane właściwości połączeń ze stali AHSS na przykładzie CPW 800*. Przegląd Spawalnictwa, 2015, vol. 87, no. 2.